AIAA JOURNAL
Vol. 47, No. 3, March 2009

Influence of Breakup Regimes on the Droplet Size Produced by Splash-Plate Nozzles

M. Ahmed* and N. Ashgriz†
University of Toronto, Toronto, Ontario M5S 3G8, Canada
and
H. N. Tran‡
University of Toronto, Toronto, Ontario M5S 3E5, Canada

DOI: 10.2514/1.36081

An experimental study was conducted to identify the influence of the breakup regime on the droplet sizes produced by a splash-plate nozzle. Sprays formed by splash-plate atomizers were categorized according to the different types of breakup regimes of a spreading liquid sheet. Mean droplet sizes of various splash-plate nozzles were determined and they were correlated to liquid viscosity, nozzle diameter, and flow velocity. Various mixtures of corn syrup and water were used to obtain viscosities in the range of 1–140 mPa · s. Three different splash-plate nozzles of 0.5, 1, and 2 mm with a constant plate angle of 55 deg were tested. A phase Doppler particle analyzer was used to determine the droplet sizes generated at various operating conditions. The results indicated that the droplet-size correlations for a splash-plate atomizer depend on the liquid-sheet breakup regime. The effect of viscosity based on power-law correlation was changed by about 2 orders of magnitudes in the exponent when the breakup regime changed from the Rayleigh–Taylor instability regime with stable rim to the sheet perforation regime.

Nomenclature

a, b, c, d, e	=	power coefficients of the correlation variables.
d_{av}	=	average droplet size, including geometrical mean (median) and arithmetic mean, mm
d_{mm}	=	mass median diameter, mm
d_{or}	=	splash-plate nozzle (orifice) diameter, mm
d_{32}	=	Sauter mean diameter, mm
n_i	=	number of droplets with a diameter d_i
Oh	=	Ohnesorge number, $\mu/(\rho\sigma d_{or})^{0.5}$
Re	=	Reynolds number, $d_{or}V\rho/\mu$
V	=	flow velocity, m/s
We	=	Weber number, $d_{or}V^2\rho/\sigma$
μ	=	liquid viscosity, Pa · s
μ_a	=	ambient air viscosity, Pa · s
ρ	=	liquid density, kg/m^3
σ	=	surface tension, N/m

I. Introduction

SPLASH-PLATE or wall-impingement nozzles are types of atomizers in which a liquid jet is obliquely impacted on a solid surface, forming a liquid sheet. The liquid sheet is later atomized into small droplets. This type of nozzle is mainly used to atomize high-viscosity liquids and when low injection pressures are needed. Wall-impinging jets are used in prefilming fuels before injection into engines and gas turbines. These splash-plate nozzles are also commonly used in boilers and furnaces to spray heavy fuel oils. Information on the droplet sizes produced by these nozzles is needed to improve design and optimize performance.

A review of the past literature on the available correlations on the mean droplet size produced by splash-plate nozzles shows that there are large discrepancies between the results. The prediction of the droplet sizes generated by splash-plate nozzles is based on the Kelvin–Helmholtz (K-H) instability theory for a liquid sheet. Dombrowski and Johns [1], Dombrowski and Hooper [2], and Fraser et al. [3] developed such a theoretical model to predict droplet sizes from the breakup of a liquid sheet. They considered effects of liquid inertia, shear viscosity, surface tension, and aerodynamic forces on the sheet breakup and ligament formation. Later, Adams [4] reduced Dombrowski and Johns's [1] model to the following correlation for the droplet size:

$$d_{mm} = 1880\mu^{0.1}V^{-0.55}d_{or}^{0.65}\rho^{-0.21}\sigma^{0.24} \tag{1}$$

where d_{mm} is the mass median diameter, defined as the droplet diameter obtained by dividing the total volume of the spray into two equal parts: one-half of the mass of the spray is contained in droplets with diameters smaller than d_{mm}, and the other half is contained in droplets with diameters larger than d_{mm}.

Bennington and Kerekes [5] developed the following empirical correlation for the Sauter mean droplet diameter generated by a splash-plate atomizer used in large boilers:

$$d_{32} = 1600\mu^{0.18}V^{-.054}d_{or}^{0.64}\rho^{0.36}\sigma^{0.18} \tag{2}$$

where d_{32} is the Sauter mean diameter, defined as the droplet diameter having the same volume/surface-area ratio as the measured droplets, where n_i is the number of droplets with a diameter d_i. They used a mixture of glycerol and water to change the fluid viscosity in the range of $\mu = 1$–15 mPa · s. Note that the diameter is correlated with viscosity according to $d_{32} \propto \mu^{0.18}$.

Empie et al. [6] reported that the average droplet size was correlated to the viscosity according to

$$d_{mm} = 5.6\mu^{0.026}V^{-0.39} \tag{3}$$

This correlation was developed for splash-plate nozzles used in Kraft recovery boilers. These boilers are used in the pulp and paper industry to burn black liquor, a byproduct of papermaking. Black liquor is a very viscous liquid and its viscosity is a strong function of temperature. Therefore, its viscosity is easily changed by changing

Received 10 December 2007; revision received 22 October 2008; accepted for publication 20 November 2008.

*Department of Mechanical and Industrial Engineering; currently Mechanical Engineering Department, Assiut University, Assiut 71516, Egypt.
†Department of Mechanical and Industrial Engineering, 5 King's College Road; ashgriz@mie.utoronto.ca (Corresponding Author).
‡Department of Chemical Engineering and Applied Chemistry, 200 College Street.

the liquor temperature. They used splash-plate nozzles with diameters of 8.5 and 9.5 mm. The viscosity of the black liquor was changed from 50 to 200 mPa · s. Note that the drop diameter relates to viscosity as $d_{mm} \propto \mu^{0.026}$.

Helpio and Kankkunen [7] measured the droplet sizes for a splash-plate nozzle with a diameter of 15–27 mm and used black liquor as the fluid with viscosities up to 65 mPa · s. They reported the following correlation:

$$d_{mm} = 1350\mu^{0.26}V^{-0.26}d_{or}^{0.74}\rho^{-0.26} \quad (4)$$

They found that diameter correlated with viscosity according to $d_{mm} \propto \mu^{0.26}$.

Inamura and Tomoda [8] and Inaumura et al. [9] investigated the behavior of a liquid sheet generated by the impingement of a liquid jet onto a solid wall. They [9] combined Dombrowski and Johns's [1] model of sheet breakup with the sheet-thickness model developed based on laminar boundary-layer analysis to predict the droplet size. However, they did not provide any correlation for droplet size. Fard et al. [10] numerically studied the effect of liquid properties and nozzle geometry on the droplet-size distribution produced by a splash-plate nozzle. Again, no correlation to relate the droplet size with the studied parameters was provided.

To conclude, there are large discrepancies among the reported correlations on the droplet size for splash-plate nozzles. The theoretical predictions show that $d_{mm} \propto \mu^{0.1}$, yet the results obtained from actual industrial nozzles show a viscosity dependency of $d_{mm} \propto \mu^{0.026}$ to $d_{mm} \propto \mu^{0.26}$. This paper is aimed at showing that such large differences may arise due to a change in the type of atomization. Therefore, we first describe different types of atomization that may exist in splash plate nozzles and then show that the droplet sizes can significantly change in different atomization regimes.

II. Experimental Setup and Procedures

Splash-plate nozzle design can have a significant effect on the shape and characteristics of the liquid sheet that it generates and, consequently, on the droplet size. To limit this effect, we have manufactured a very simple splash-plate nozzle. A cross-sectional view of this nozzle is shown in Fig. 1. This nozzle is constructed by machining an aluminum rod of length A such that a pipe with an inner diameter of d_{or} is first formed (this is the nozzle diameter). The rod is then machined through its cross section at a 55 deg angle to clear the pipe opening. Three different nozzle diameters (0.5, 1, and 2 mm) were used. All aspect ratios of the nozzles are geometrically scaled according to the nozzle diameters, and the splash-plate angle was kept constant at 55 deg.

Solutions of corn syrup with water were used to obtain a wide range of viscosities, ranging from 1.0 to 140 mPa · s. Viscosities were measured using a Rheometrics ARES-RFS3 mechanical spectrometer using a 50 mm cone and plate geometry. By knowing the density of the corn syrup at room temperature ($\rho = 1450$ kg/m^3), densities of the solutions of corn syrup and water were calculated. In addition, the surface tension of the solution was measured using a Kruss K100MK2 tensiometer. The flow velocities in the splash-plate nozzle ranged from 7 to about 62 m/s. A rotameter was used to measure the flow rate of the liquid from the pressurized tank to the splash-plate nozzle. Two rotameters were used to measure flows in the range of 0.1 to 1.8 liters/min and 2.0 to 7.0 liters/min. For solutions of water and corn syrup, a graded cylinder and stopwatch were used to measure the flow rate by collecting a certain volume of solution over a known time. The uncertainty in the flow rate measurements is less than 2.0%. Physical properties of the corn syrup solutions used are shown in Table 1.

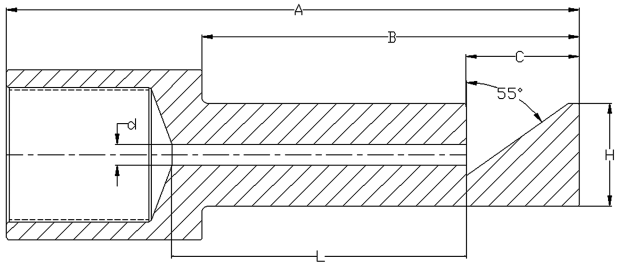

Fig. 1 A Sectional view of splash-plate nozzles with different diameters (d = 0.5, 1.0, and 2 mm).

Table 1 Properties of various mixtures of corn syrup and water

	Mixing ratio by volume, water to corn syrup		
	1:1	1:2	1:3
Viscosity, mPa · s	12	65	140
Density, kg/m^3	1225	1300	1335
Surface tension, N/m	0.067	0.066	0.068
Refraction index	1.4125	1.437	1.449

The splash-plate nozzle was connected to a pressure tank through a flow meter. A constant pressure supply of compressed nitrogen was used via a pressure regulator to pressurize a solution of corn syrup and water inside the tank. A two-dimensional phase Doppler particle analyzer (PDPA) from TSI, Inc., was used to determine droplet-size distributions. Regarding the phase-receiver optics, the focal length of the front lens and the back lens was fixed and equal to 750 and 250 mm, respectively. However, the focal length of the transmitter lens was variable and depended on nozzle diameter. For 0.5 and 1.0 mm nozzles, the focal length was 512 mm. When the nozzle diameter was increased to 2 mm, the spray droplets became larger, and the focal length of 762 mm was consequently used. The offset angle of 60 deg was selected and fixed for all operating conditions in which a 60- deg receiver angle is not ideal for PDPA setup to measure transparent droplets. The splash plate of the nozzle was placed vertically. To increase the accuracy of measurements, approximately 10,000 droplets were measured in each run to establish the droplet-size distributions. For each run, three replications were conducted and the average value of the Sauter mean diameter d_{32} was considered [11]. The measurements were performed at a distance of 100 times the orifice diameter (100 d_{or}) from the splash-plate nozzle tip along the centerline of the spray sheet. Therefore, the droplet-size information provided here is representative of the droplets at the spray center. The Dantec PDPA manual [12] gives the uncertainty of the PDPA measurements. The uncertainty in the droplet-size measurements is less than 5%.

III. Results and Discussion

An extensive set of experimental data is obtained on splash-plate nozzle sprays. It is found that different breakup mechanisms govern the spray formation for certain ranges of operating parameters. Therefore, droplet-size correlations should consider the specific breakup mechanism. A detailed description of the splash-plate breakup mechanism is given elsewhere [13,14] and only a brief review is provided in Sec. III.A. Various correlations for the mean droplet size are provided in Sec. III.B. Finally, effects of liquid viscosity, nozzle diameter, and flow velocity on the mean droplet size are discussed in Sec. III.C.

A. Breakup Mechanism

The breakup mechanisms for the sheet produced by a splash-plate nozzle were studied using direct imaging techniques. It was found that the sheet breakup process for the range of variables studied is governed by three different mechanisms: Rayleigh–Plateau (R-P) and Rayleigh–Taylor (R-T) instabilities and sheet perforation. R-P occurs at the rim of the sheet [15,16], whereas R-T occurs on the thin liquid sheet. Previous theoretical models have used K-H instability to describe the atomization of a liquid sheet. However, for the range of parameters used in all of our experiments, K-H instability was not the dominant mechanism of the sheet breakup. The experiments showed that the sheet became thin and perforated. The sheet then retreated from the perforation zone and broke into small droplets. This type of breakup more resembled R-T instability than K-H instability.

a) Stable rim and laminar R-T instability on the sheet breakup regime

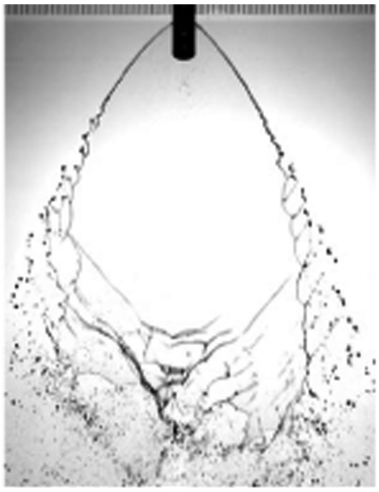

b) Laminar R-P instability at the rim and laminar R-T instability on the sheet breakup regime

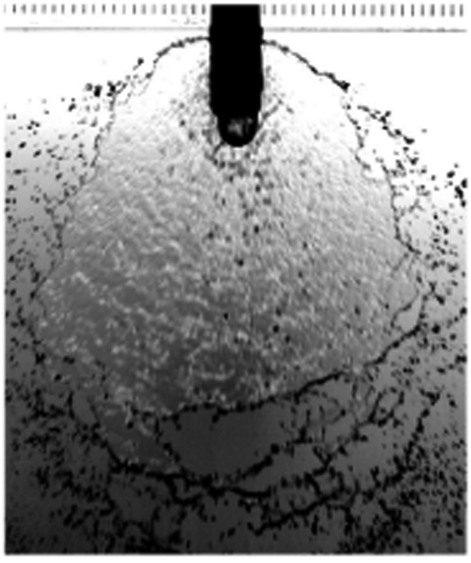

c) Turbulent R-P instability at the rim and turbulent R-T instability on the sheet breakup regime

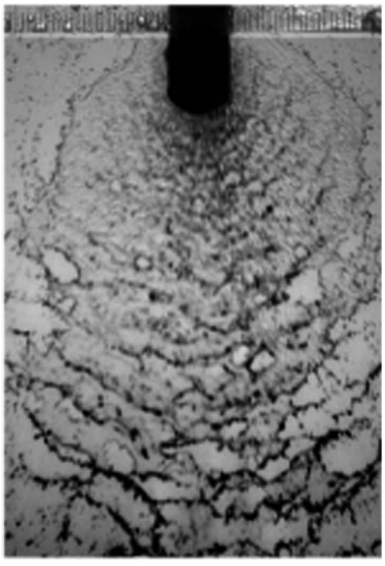

d) Perforation regime

Fig. 2 Sheet breakup regimes.

The R-T instability of the sheet is always observed at the outer edges of the radially spreading sheet, where the sheet is the thinnest. It can also occur inside the sheet, due to formation of holes and ruptures. The rim instability can be laminar or turbulent, depending on the jet Reynolds number. Further details regarding the breakup process are given by Ahmed et al. [13]. Figure 2 shows the breakup mechanism for the range of variables studied here. Sheet breakup due to R-T sheet instability is depicted in Fig. 2a and is defined as stable rim and laminar R-T instability on the sheet breakup regime. Based on this figure, large surface waves are formed on the sheet. The sheet is, in general, very thin, except for the edges or rims. This thin sheet can easily be disturbed by the surrounding air. As the surface waves grow, they stretch the sheet and make it thinner, until it ruptures. Once the sheet ruptures, it retreats backward at a rapid rate. This results in a Rayleigh–Taylor type of instability.

Figure 2b shows the sheet breakup process due to a laminar R-P instability at the rim and a laminar R-T instability on the sheet. The shape of the liquid sheet is determined based on the competition between the momentum and the surface-tension forces at the sheet boundaries. Once the droplets are pinched off of the rim, they may still be attached to the sheet. As the sheet retreats at a rapid rate, it cannot pull the relatively large droplet along with it. Therefore, a thin liquid ligament forms that keeps the sheet and the droplet attached. Later, this ligament becomes unstable and breaks off into several small drops and releases the main droplet. The rim of the sheet acts as a curved liquid jet. According to Rayleigh [17], any perturbation with a wavelength greater than the perimeter of the jet will grow and make the jet unstable (i.e., R-P instability). Consequently, the rim can become unstable and generate droplets if R-P instability conditions are satisfied, as shown in Fig. 2b. However, for higher viscosity and a low Reynolds number, the sheet rim is always stable, as shown in Fig. 2a.

Figure 2c shows sheet breakup process due to a turbulent R-P instability at the rim and a turbulent R-T instability on the sheet. In this regime, the droplets are formed mainly from the turbulent edges of the sheet. Perturbations in the sheet are attributed to the turbulent flow inside the splash-plate nozzle. Figure 2d shows the perforation regime. In this regime, the spreading angle is close to 180 deg, due to low viscosity effect, and the Reynolds number is much higher than with the previous regime. This leads to highly local disturbances in the sheet that result in the formation of perforations near the nozzle exit.

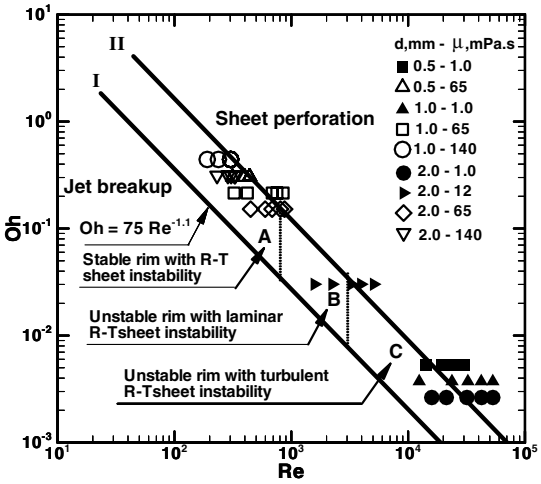

Fig. 3 Breakup regimes at different values of Reynolds and Ohnesorge numbers.

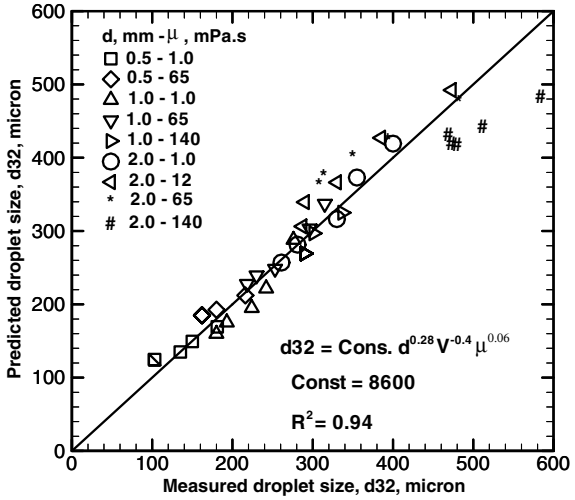

Fig. 4 Variation of the measured average droplet size d_{32} and the predicted values for all breakup regimes (regions A, B, and C and sheet perforation).

Breakup regimes can be identified on a Reynolds Re versus Ohnesorge Oh number plane, as shown in Fig. 3. Three main regions are identified in Fig. 3. In the region below line I, identified as the *jet breakup region*, there is no sheet formation and only a liquid jet is formed, which later breaks up into droplets. The empirical equation, as defined in [13] for line I, can be written as

$$Oh = \frac{75}{Re^{1.1}} \tag{5}$$

Above line 1, a liquid sheet is formed, which later breaks up into droplets. Line II divides the sheet breakup into two types. Below line II and above line I, the sheet does not have any perforations, whereas above line II, sheet breakup is dominated by perforation breakup. The region between lines I and II can be divided into three zones, as stated in the figure, and represent three breakup regimes: stable rim with R-T sheet instability (region A), unstable (laminar) rim with laminar R-T sheet instability (region B), and unstable (turbulent) rim with turbulent R-T sheet instability (region C).

B. Droplet-Size Correlations

Sprays produced by a splash-plate nozzle are characterized in terms of the following parameters: 1) characteristic dimensions of the splash-plate nozzle (e.g., nozzle diameter d_{or}, nozzle length L, flow velocity V, and plate angle α, as defined in Fig. 1; 2) physical properties of liquid such as viscosity μ, density ρ, and surface tension σ; 3) physical properties of the ambient air such as air viscosity μ_a and air density ρ_a; and 4) liquid and ambient temperatures. We have used only one nozzle plate angle of 55 deg. In addition, the ambient conditions are kept at atmospheric conditions and the effect of temperature and ambient air velocities are not considered. Three different liquid viscosities of 1, 65, and 140 mPa · s and three different nozzle diameters of 0.5, 1, and 2 mm are considered.

1. *Droplet-Size Correlation for All Breakup Regimes*

The following correlation is obtained using the data from all test cases, regardless of the type of atomization:

$$d_{32} = 8.6\mu^{0.06}V^{-0.4}d_{\text{or}}^{0.28} \tag{6}$$

where d_{32} is defined as the Sauter mean diameter [11]. The regression coefficient for this correlation is $R^2 = 0.94$. Figure 4 presents this correlation for the range of liquid viscosities, nozzle diameters, and flow velocities of all breakup regimes that are considered here. It is shown that the droplet size is a weak function of viscosity, $d_{32} \propto \mu^{0.06}$, and a strong function of flow velocity and orifice diameter.

2. *Droplet-Size Correlations for the Transition and Perforation Regimes*

The transition regime is the region between lines I and II in Fig. 3: namely, regions A, B, and C on this figure. The droplet-size correlation for both cases can be written as follows.

For the sheet breakup regime:

$$d_{32} = 8.27\mu^{0.09}V^{-0.52}d_{\text{or}}^{0.22} \quad \text{with} \quad R^2 = 0.94 \tag{7}$$

For the sheet perforation regime:

$$d_{32} = 8.14\mu^{0.003}V^{-0.35}d_{\text{or}}^{0.36} \quad \text{with} \quad R^2 = 0.96 \tag{8}$$

Figures 5a and 5b show the preceding correlations. In the first correlation, the droplet size is a much stronger function of viscosity, $d_{32} \propto \mu^{0.09}$, than the second correlation, $d_{32} \propto \mu^{0.003}$. This clearly indicates a need for including the type of sheet breakup in any droplet-size correlation.

3. *More Refined Droplet-Size Correlations*

The droplet-size correlation can be further divided into other breakup regimes, identified on Fig. 3. The following correlation is developed based on using only the data from the R-T sheet instability breakup regime (region A in Fig. 3.):

$$d_{32} = 13.57\mu^{0.27}V^{-0.48}d_{\text{or}}^{0.24} \quad \text{with} \quad R^2 = 0.97 \tag{9}$$

The following correlation is obtained based on using the data from the unstable rim with laminar R-T sheet instability and unstable rim with turbulent R-T sheet instability regimes (regions B and C in Fig. 3):

$$d_{32} = 3.11\mu^{0.07}V^{-0.5}d_{\text{or}}^{0.1} \quad \text{with} \quad R^2 = 0.99 \tag{10}$$

Equation (8) was provided for the perforation regime. Figure 6 shows the correlation for the three breakup regimes. The first breakup regime is defined as the R-T sheet instability regime, as shown in Fig. 6a. The second regime includes the unstable rim with laminar R-T sheet instability and unstable rim with turbulent R-T sheet instability regimes, as shown in Fig. 6b. The last regime is due to sheet perforation, as shown earlier in Fig. 5b. In the R-T sheet instability breakup regime (region A), there is a strong dependence between the droplet size and the liquid viscosity, $d_{32} \propto \mu^{0.27}$. However, in the unstable rim with laminar R-T sheet instability and unstable rim with turbulent R-T sheet instability regimes (regions B and C in Fig. 3), there is a weaker dependence on viscosity, $d_{32} \propto \mu^{0.07}$. Also, as previously indicated, in the perforation regime, the droplet size is a very weak function of viscosity, $d_{32} \propto \mu^{0.003}$.

Note that the effect of density and surface tension is not included in the preceding correlations, because their variations in the current

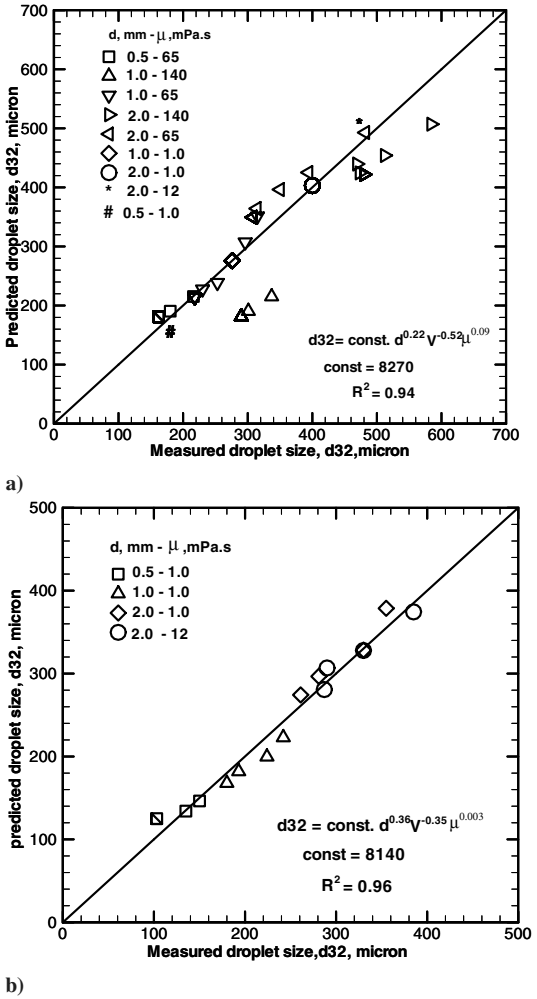

Fig. 5 Variation of the measured average droplet size d_{32} and the predicted values for a) regions A, B, and C in Fig. 3, and b) the sheet perforation regime.

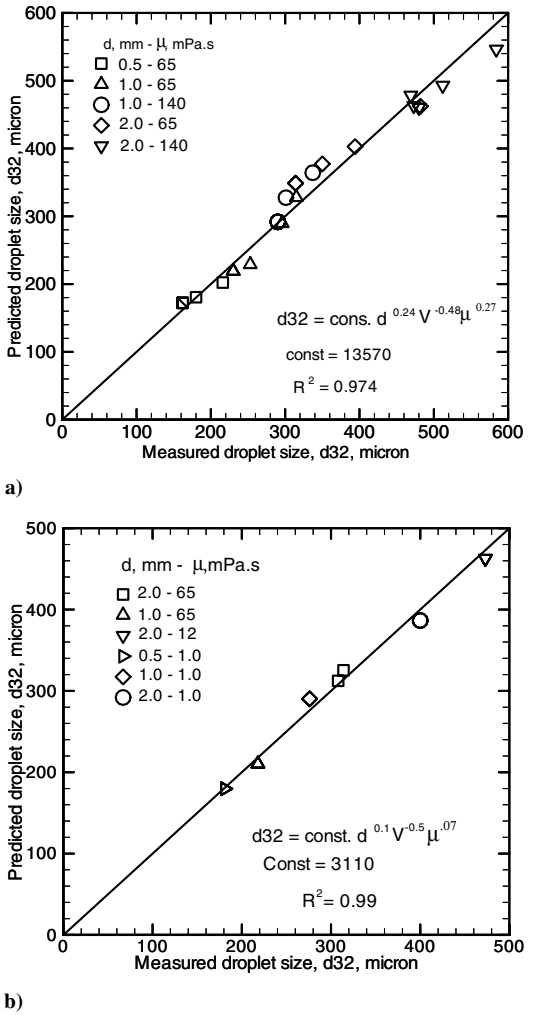

Fig. 6 Variation of the measured average droplet size d_{32} and the predicted values for a) the R-T sheet instability regime and b) unstable rim with laminar R-T sheet instability and unstable rim with turbulent R-T sheet instability regime.

experiments were small (i.e., density was changed from 1000 to 1335 kg/m^3, and surface tension was changed from 0.066 to 0.072 N/m). Also, note that the unstable rim with laminar R-T sheet instability breakup regime (region B) and unstable rim with turbulent R-T sheet instability regime (region C) are considered as one breakup regime, because there were not enough data points to obtain separate correlates for each. The comparison between the present correlations and those given in the literature is shown in Table 2.

The corresponding nondimensional correlations based on Reynolds number, Weber number, and viscosity ratio were obtained. The effect of density ratio was ignored due to small changes in the values of liquid density.

For all breakup regimes, droplet-size correlation was found to be as follows:

$$\frac{d_{32}}{d_{\text{or}}} = 28.6 \times 10^3 Re^{-1.02} We^{0.3} \left(\frac{\mu}{\mu_a}\right)^{-0.91} \quad \text{with} \quad R^2 = 0.89 \tag{11}$$

For different flow regimes, the correlations were found to be as follows:

For the sheet perforation regime,

$$\frac{d_{32}}{d_{\text{or}}} = 12.4 \times 10^3 Re^{-0.94} We^{0.29} \left(\frac{\mu}{\mu_a}\right)^{-0.89} \quad \text{with} \quad R^2 = 0.90 \tag{12}$$

Table 2 Comparisons between the present and previous correlations of droplet size $d_{32} = C\mu^a V^b d^c \rho^d \sigma^e$

Reference[a]	Liquid	a	b	c	d	e	Comments
Dombrowski and Johns [1]	Theory	0.1	−0.55	0.65	−0.21	0.24	Sheet instability model
Bennington and Kerekes [5]	Glycerol and water	0.18	−0.54	0.64	−0.36	0.18	$d = 0.7$ mm, $\mu = 1$–15 mPa · s
Empie, et al. [6]	B.L.	0.026	−0.39	——	——	——	$d = 8.5$–9.5 mm, $\mu = 50$–200 mPa · s
Helpio and Kankkunen [7]	B.L.	0.26	−0.26	0.74	−0.26	——	$d = 15$–27 mm, $\mu = 1$–15 mPa · s
Present work (all regimes)	Corn syrup	0.06	−0.4	0.28	——	——	$d = 0.5$–1.0 mm, $\mu = 65$–140 mPa · s
Present work (A, B, and C regimes)	Corn syrup	0.09	−0.52	0.22	——	——	$d = 0.5$–2.0 mm, $\mu = 1.0$–140 mPa · s
Present work (perforation regime)	Corn syrup	0.003	−0.35	0.36	——	——	$d = 0.5$–2.0 mm, $\mu = 1.0$–140 mPa · s
Present work (B and C regimes)	Corn syrup	0.07	−0.5	0.1	——	——	$d = 0.5$–2.0 mm, $\mu = 1.0$–140 mPa · s
Present work (A regime)	Corn syrup	0.27	−0.48	0.24	——	——	$d = 0.5$–2.0 mm, $\mu = 1.0$–140 mPa · s

[a]Regime A is defined as R-T sheet instability, regime B is defined as an unstable rim with laminar R-T sheet instability, and regime C is defined as an unstable rim with turbulent R-T sheet instability.

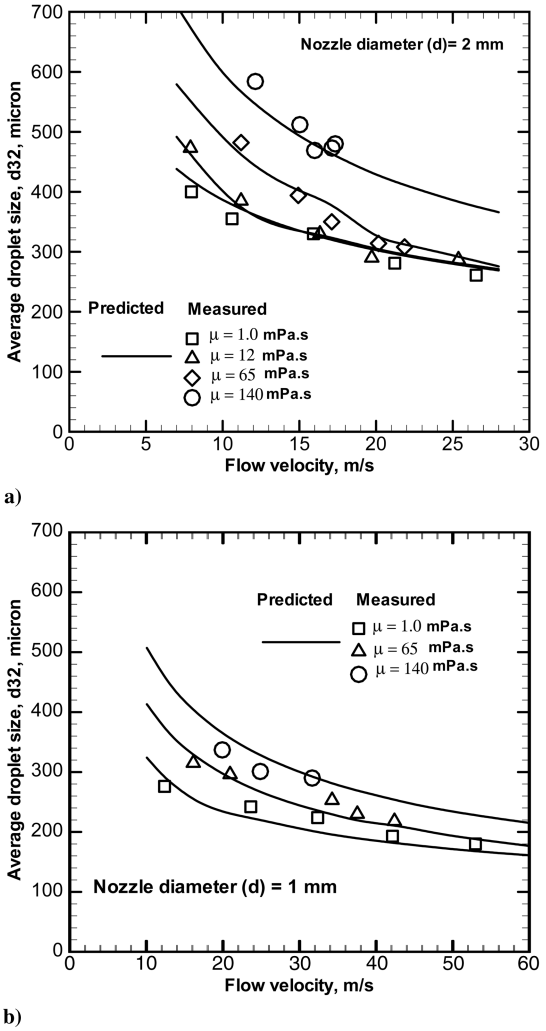

Fig. 7 Variation of average droplet size versus flow velocity at different values of viscosity.

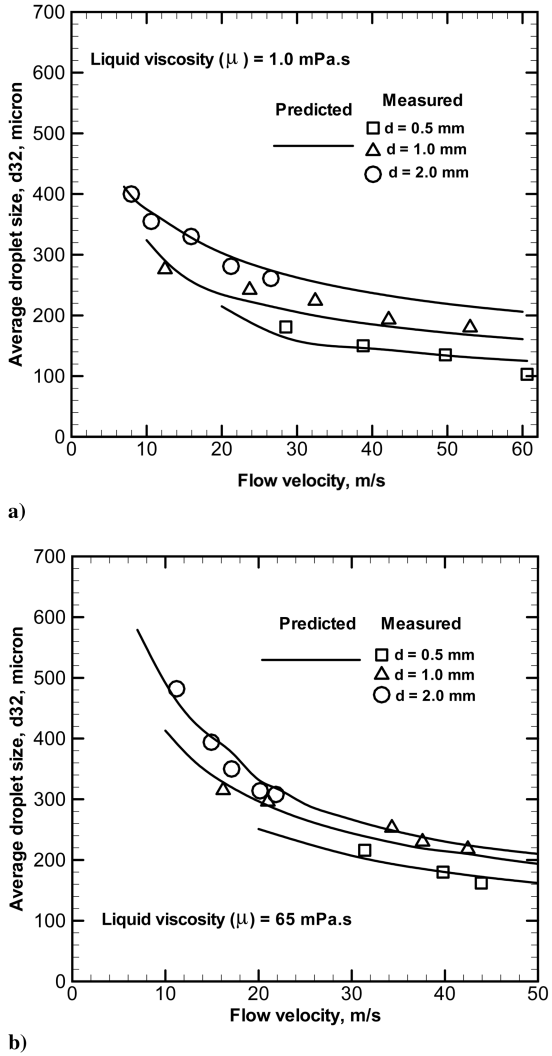

Fig. 8 Variation of average droplet size versus flow velocity at different values of nozzle diameter.

For the R-T sheet instability breakup regime (region A in Fig. 3.),

$$\frac{d_{32}}{d_{\text{or}}} = 7.1 \times 10^3 Re^{-1.04} We^{0.28} \left(\frac{\mu}{\mu_a}\right)^{-0.72} \quad \text{with} \quad R^2 = 0.94 \tag{13}$$

For the unstable rim with laminar R-T sheet instability and unstable rim with turbulent R-T sheet instability regimes (regions B and C in Fig. 3),

$$\frac{d_{32}}{d_{\text{or}}} = 507 \times 10^3 Re^{-1.28} We^{0.40} \left(\frac{\mu}{\mu_a}\right)^{-1.16} \quad \text{with} \quad R^2 = 0.99 \tag{14}$$

Most droplet-size correlations are expressed based on nondimensional groups. This type of correlation function is valid for a wide range of nozzle design and fluid properties. However, correlations based on dimensional variables better describe the effect of each variable within each breakup regime.

C. Effect of Liquid Viscosity, Nozzle Diameter, and Flow Velocity on Droplet Size

Figure 7 shows the variation of droplet size with flow velocity at two different nozzle diameters: 2 and 1 mm. Figure 7a shows the behavior of d_{32} with viscosity for a 2 mm splash-plate nozzle. For this case, the average droplet size increases with increasing the viscosity at all values of flow velocity. The same trend is shown in the case of a 1 mm nozzle diameter, as shown in Fig. 7b. Increasing the viscosity results in an increase in the resistance of liquid to spreading and, consequently, a reduction in the sheet spreading angle. This will lead to an increase in the sheet thickness and, consequently, an increase in the droplet size.

Three different nozzle diameters (0.5, 1, and 2 mm) were selected to investigate the effect of nozzle diameter on the average size. Figure 8 presents the variation of the average droplet size versus the flow velocity at different nozzle diameters for two different values of viscosities: 1.0 mPa · s in Fig. 8a and 65 mPa · s in Fig. 8b. It was found that increasing the nozzle diameter results in a significant increase in the average droplet size. Increasing the nozzle diameter at a constant flow velocity results in an increase in the flow rate; consequently, the liquid sheet becomes thicker and breaks into larger droplets.

The effects of increasing the flow rate on the average droplet size at different nozzle diameters and viscosities are shown in Figs. 7 and 8. It is clear, based on these figures, that after increasing the flow velocity, the average droplet size decreases for all nozzles diameters as well as liquid viscosities. An increase in the flow velocity reflects an increase in the energy available for the breakup. Increasing the atomization energy results in smaller droplet sizes. Note that the nonsmooth behavior of the predicted droplet size at the viscosities of 12, 65, and 140 mPa · s in Fig. 7a is mainly due to the transition from one breakup regime to another. Similar behavior was also shown in Fig. 8b in the case of a nozzle diameter of 2.0 mm.

IV. Conclusions

The factors affecting the droplet size produced by a splash-plate nozzle were investigated at different operating nozzle conditions.

Corn syrup was used as the working fluid. Measurements of the spray characteristics were conducted for small-scale nozzles. Droplet-size measurements were performed using a phase Doppler particle analyzer. An empirical correlation of droplet size with nozzle operating conditions was developed for three different breakup mechanisms. The results can be summarized as follows.

Droplet-size correlation for splash-plate nozzles should include the type of liquid atomization. A single correlation cannot accurately present the variation of droplet size with independent variables, whether these variables are presented in dimensional or nondimensional form. It is more accurate to use different droplet-size correlations for each type of breakup regime: 1) stable rim and laminar R-T instability on the sheet breakup regime, 2) laminar R-P instability at the rim and laminar R-T instability on the sheet breakup regime, 3) turbulent R-P instability at the rim and turbulent R-T instability on the sheet breakup regime, and 4) perforation breakup regime.

Droplet size is strongly affected by liquid viscosity, $d_{32} \propto \mu^{0.27}$, at a low Reynolds number and a high Ohnesorge number ($Re \leq 800$ and $Oh \geq 0.22$); it is moderately dependent on viscosity, $d_{32} \propto \mu^{0.07}$, at moderate Reynolds and Ohnesorge numbers ($800 \leq Re \leq 3000$ and $0.03 \leq Oh \leq 0.22$), whereas it is weakly dependent on viscosity, $d_{32} \propto \mu^{0.003}$, at high Reynolds and low Ohnesorge numbers ($Re \geq 18,000$ and $Oh \leq 0.003$). The exponents of the main variables (flow velocity V, nozzle diameter d_{or}, and liquid viscosity μ) on correlations based on dimensionless variables are approximately the same as those developed based on dimensional variables.

Nozzle diameter has a significant effect on the average droplet size. Increasing the nozzle diameter causes an increase in the average droplet size for all breakup regimes. Increasing flow velocity results in a significant decrease in the average droplet size, due to increasing the applied energy for the breakup process for all regimes.

References

[1] Dombrowski, N., and Johns, W., "The Aerodynamic Instability and Disintegration of Viscous Liquid Sheets," *Chemical Engineering Science*, Vol. 18, No. 3, 1963, 203–213. doi:10.1016/0009-2509(63)85005-8

[2] Dombrowski, N., and Hooper, P. C., "A Study of Spray Formed by Impinging Jets in Laminar and Turbulent Flow," *Journal of Fluid Mechanics*, Vol. 18, No. 3, 1964, 392–440. doi:10.1017/S0022112064000295

[3] Fraser, R., Eisenklam, P., Dombrowski, N., and Hasson, D., "Drop Formation from Rapidly Moving Liquid Sheets," *AIChE Journal*, Vol. 8, No. 5, 1962, 672–680. doi:10.1002/aic.690080522

[4] Adams, T., *Kraft Recovery Boilers*, TAPPI Press, Atlanta, 1997, Chap. 4.

[5] Bennington, C., and Kerekes, R., "The Effect of Temperature on Drop Size of Black Liquor Sprays," *Journal of Pulp and Paper Science*, Vol. 12, No. 6, 1986, pp. J181–J186.

[6] Empie, H., Lien, S., and Yang, W., "Effect of Black Liquor Type on Droplet Formation from Commercial Spray Nozzles," *Journal of Pulp and Paper Science*, Vol. 21, No. 2, 1995, J63–J67.

[7] Helpio, T., and Kankkunen, A., "The Effect of Black Liquor Firing Temperature on Atomization Performance," *TAPPI Journal*, Vol. 79, No. 9, 1996, 158–163.

[8] Inamura, T., and Tomoda, T., "Characteristic of Spray Through Wall Impinging Nozzles," *Atomization and Sprays*, Vol. 14, 2004, pp. 375–395. doi:10.1615/AtomizSpr.v14.i4.40

[9] Inamura, T., Yanaoka, H., and Tomoda, T., "Prediction of Mean Droplet Size of Sprays Issued from Wall Impingement Injector," *AIAA Journal*, Vol. 42, No. 3, 2004, pp. 614–621. doi:10.2514/1.9112

[10] Fard, M. P., Levesque, D., Morrison, S., Ashgriz, N., and Mostaghimi, J., "Characterization of Splash Plate Atomizers Using Numerical Simulations," *Atomization and Sprays*, Vol. 17, No. 4, 2007, pp 347–380. doi:10.1615/AtomizSpr.v17.i4.30

[11] Lefebvre, A. H., *Atomization and Sprays*, Hemisphere, New York, 1989.

[12] *Dantec PDPA Manual*, Dantec Corp., Skovlunde, Denmark, 1995.

[13] Ahmed, M., Amighi, A., Ashgriz, N., and Tran, H., "Characteristics of Liquid Sheets Formed by Splash-Plate Nozzles," *Experiments in Fluids*, Vol. 44, No. 1, 2008, pp 125–136. doi:10.1007/s00348-007-0381-4

[14] Ahmed, M., Ashgriz, N., and Tran, H., "Break-Up Length and Spreading Angle of Liquid Sheets Formed by Splash Plate Nozzles," *Journal of Fluids Engineering*, Vol. 131, 2009, Paper 011306. doi:10.1115/1.3026729

[15] Li, R., and Ashgriz, N., "Characteristics of Liquid Sheets Formed by Two Impinging Jets," *Physics of Fluids*, Vol. 18, No. 8, Paper 087104. doi:10.1063/1.23380642006.

[16] Li, R., and Ashgriz, N., "Edge Instability and Velocity of Liquid Sheets Formed by Two Impinging Jets," *Atomization and Sprays*, Vol. 17, No. 1, pp. 71–91. doi:10.1615/AtomizSpr.v17.i1.302007.

[17] Rayleigh, L., "On the Instability of Jets," *Proceedings of the London Mathematical Society*, Vol. 10, 1879, pp. 4–13.

R. Rangel
Associate Editor